

Toward Wearable Sensors: Fluorescent Attoreactor Mats as Optically Encoded Cross-Reactive Sensor Arrays**

Pavel Anzenbacher Jr.,* Fengyu Li, and Manuel A. Palacios

Herein we demonstrate the fabrication of high-density attoreactor sensor arrays for the detection of metal ions. Recently, we developed a method of synthesis of ultra-small amounts of products, down to zeptomol (zmol, 10^{-21} mol) amounts confined in junctions of polymer nanofibers.^[1] This method is well suited for the synthesis of fluorescent materials. The electro-spun nanofibers^[2] give porous mats that comprise fluorescent attoliter-sized junctions termed attoreactors that give off bright fluorescence (Figure 1), and form almost conformal coating on various surfaces. Moreover, the highly porous electrospun nanofiber mats facilitate sensor-analyte mass exchange, which results in short response times. Such mats with embedded in situ formed fluorescent “attosensors” generate high-density and parallel sensor arrays.^[3] Furthermore, the key feature of attosensor array mats, when compared to sensor films based on bulk material, is that approximately a 1000 of molecules can be positioned in a small volume (attoliters), thus concentrating the fluorescence of probe molecules that are easy to detect with optical microscopy.^[1]

Cation recognition and detection, particularly of heavy metals,^[4] has an enormous potential environmental and health-related impact.^[5] Herein, we explore the possibility of synthesizing fluorescent sensors within one nanofiber mat, which would then serve as an optically encoded (wavelength-addressable) cross-reactive attosensor array. We demonstrate this approach on sensing a benchmark group of ten metal ions (Al^{3+} , Fe^{3+} , Co^{2+} , Ni^{2+} , Cu^{2+} , Zn^{2+} , Hg^{2+} , Cd^{2+} , Ca^{2+} , Mg^{2+}). This method can be, however, used for other analytes as well.

First, we show the ability of a single attoreactor to act as a fluorescent sensor. Here, we use fluorophore-polyamines (e.g. dansyl-polyamines)^[6] that bind metal ions while displaying a change in fluorescence. Figure 2 shows three polyurethane nanofibers: Two are doped with triethylenetetramine (4N) and one with dansyl chloride (bottom left → top right), forming two fluorescent attoreactors. One attoreactor (lower left) serves as a reference while the other is used as a sensor. The images show the attosensors before and after adding a droplet of aqueous CoCl_2 , and after washing away the CoCl_2 with water. The fluorescence from the reference reactor did not change appreciably throughout the experiment. The exposure of the attosensor to CoCl_2 resulted in fluorescence

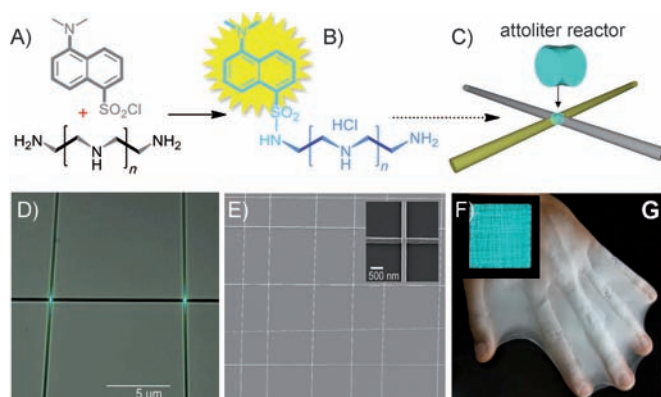


Figure 1. Overlap of two types of polymer nanofibers (300 ± 50 nm diam.), each carrying a different reagent, for example, dansyl chloride and polyamine (A), to produce fluorescent products (B) in the fiber junctions, attoliter volume reactors comprising zeptomol amounts of fluorescent products (C, D) in the form of a highly porous mat (E) that can be deposited by a shadow mask (F) on a variety of surfaces (G).

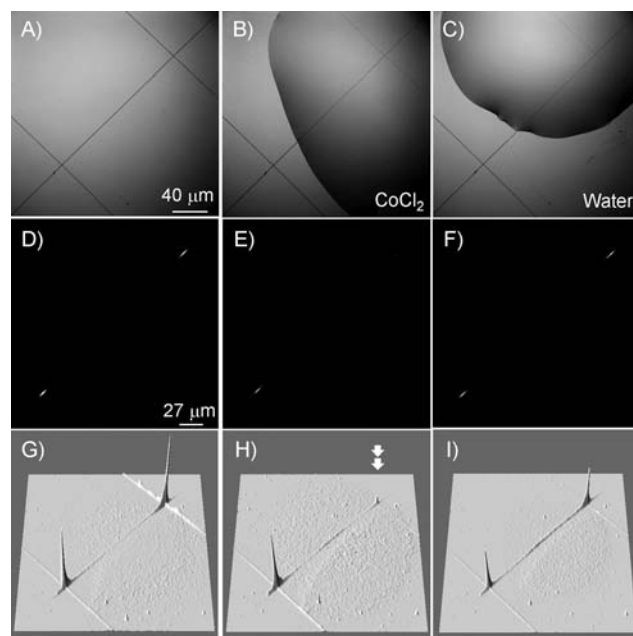


Figure 2. Self-referencing attosensor: One reactor (lower left) is used as a reference, while the other is used as Co^{2+} ion sensor. Top: Bright-field images before (A) and after (B) addition of CoCl_2 , and after regenerating the sensor with nanopure water (C). Corresponding fluorescence images (D–F). Bottom: the 3D representation of the integrated fluorescence intensity (G–I) corresponding to D–F.

[*] P. Anzenbacher Jr., F. Li, M. A. Palacios
Department of Chemistry, Bowling Green State University
Bowling Green, OH 43403 (USA)
E-mail: pavel@bgsu.edu

[**] P.A. acknowledges support from BGSU and the NSF (CHE-0750303, DMR-1006761).

Supporting information for this article is available on the WWW under <http://dx.doi.org/10.1002/anie.201105629>.

quenching. The fluorescence was recovered upon washing with water. This observation confirms the ability of the attoreactors to act as sensors that can be generated in situ and bind metal ions in a reversible fashion (4 cycles).

In the future, the analytical potential of the attosensor mats could be expanded to become a massively parallel sensing array by reading one or few individual attoreactors (from a mat comprising approximately 10^7 attosensors). While this qualitative test was performed at a high analyte concentration (200 μM , 200 nL, pH 5), it can be performed at a concentration as low as 5 ppm. One of the advantages of the present approach is the possible use of small samples (down to pL) obtained by concentrating diluted samples. In any case, owing to the density of the nanofiber mat, there will be approximately 10^4 individual attoliters sensors under every 10 nL droplet. Importantly, nanofiber mats can comprise more than two reagents. We tested a nanomat composed of four different nanofibers: A fiber doped with an amine such as tetraethylene pentamine (5N), another one with dansyl chloride (DS), one with fluorescamine (FL, Fluram), and one with 7-chloro-4-nitrobenz-2-oxa-1,3-diazole (NBD).

None of these four chemicals are fluorescent, but the products of the reaction of the fluorophore precursors (DS, FL, NBD) with the amine are. Thus, the dansylated pentamine displays cyan emission ($\lambda_{\text{max}} = 480 \text{ nm}$, $\tau = 7.85 \text{ ns}$), the Fluram-amine product shows blue emission ($\lambda_{\text{max}} = 465 \text{ nm}$, $\tau = 2.80 \text{ ns}$), and the NBD-amine a green emission ($\lambda_{\text{max}} = 525 \text{ nm}$, $\tau = 3.87 \text{ ns}$), Figure 3 A–E.

The in-situ-synthesized probes may be generated in the nanofiber mat to match the analyte composition. In an even more general sense, the amounts of the label–receptor probes may be adjusted on demand to satisfy the requirements for excitation/emission wavelengths, amount, and concentration of the analyte, etc. Figure 3F shows nine probes (3×3) with DS–5N, FL–5N, and NBD–5N as well as zoomed-in images of each junction type to show the difference in fluorescence output. The three probes, DS–5N, FL–5N, and NBD–5N, have different affinity to metal ions. This is because, for example, FL–5N comprises a carboxylate group that may participate in the metal ion binding, while the nitrogen atom in the oxadiazole ring of NBD–5N may participate in the formation of the probe–ion complex, or because the sulphonamide oxygen in the DS–5N may interact with oxophilic cations, etc. Similarly, a varying of the ethylene amines (4N, 5N, 6N) introduces a variable likely to induce a different response to different metal ions.

In the attosensor mat, the amine-bearing and fluorophore-precursor-doped nanofibers are deposited at an angle of approximately 90° to form a rectangular grid (Figure 3A,F). The location of the respective DS, FL, NBD fibers is, however, random. Thus, the location of the in-situ generated probes within the grid is random as the junctions with blue/cyan/green emission are not formed in an exact pre-defined location. This is, however, not a hindrance because the probes are optically encoded with their specific emission profiles.

While the individual attosensors operate independently (on a microscopic level, Figure 2), in practice, the fluorescence is recorded from the whole mat ($12 \times 12 \text{ mm}$) compris-

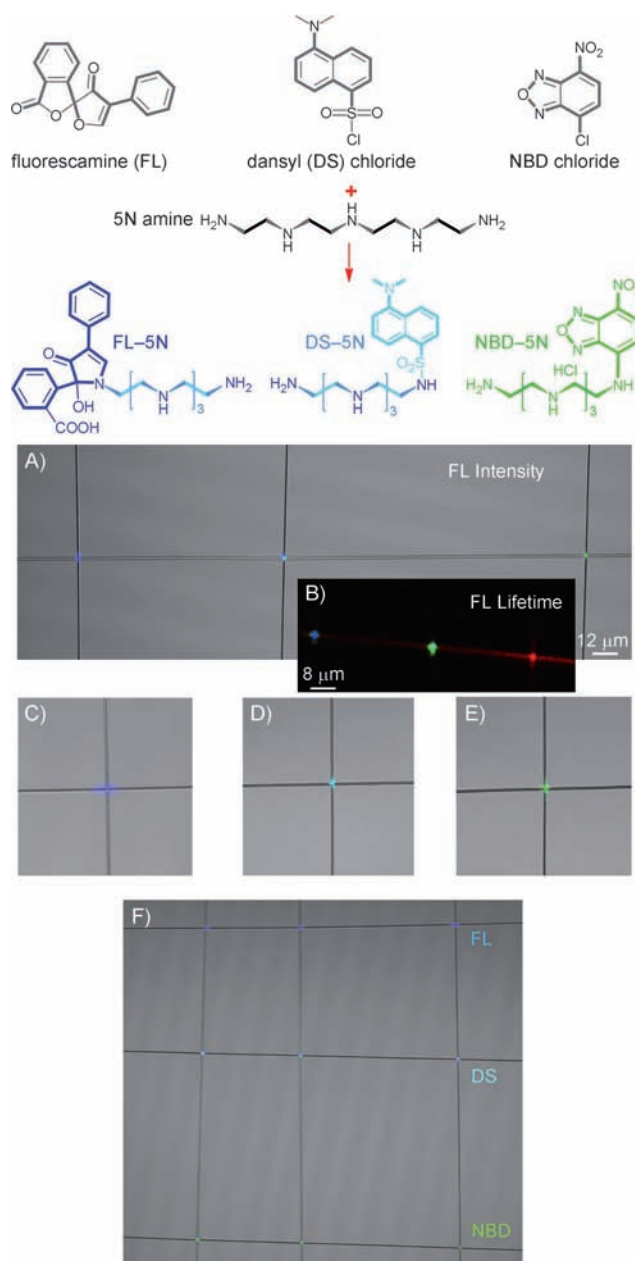


Figure 3. The reaction of fluorophore precursors (DS, FL, NBD) with tetraethylene pentamine in situ (i.e. in the nanofiber junctions) results in fluorescent products. The color of emission (fluorescence image is superimposed on a bright-field image) corresponds to the images above (A). The emission can be observed as an image based on fluorescence lifetime (B), so called fluorescence lifetime (FLIM) image. The virtual sensor array comprising in situ prepared fluorescent probes DS–5N, FL–5N, and NBD–5N (F). The three probes, FL–5N (C), NBD–5N (D), and DS–5N (E), were synthesized from pentamine-doped polyurethane fibers (vertical) and the fluorophore precursors in the horizontal direction. The images are bright-field images with superimposed confocal fluorescence images.

ing all the probes (Figure 3). The metal sensing data were acquired from analyte droplets (0.2 μL) deposited on the mat together with a reference sample (water, pH 5). The drops were allowed to dry prior to fluorescence measurement using a UV/vis scanner (excitation at ca. 365 nm) that records

fluorescence response using four emission channels ($\lambda_1 = 440$ nm, $\lambda_2 = 480$ nm, $\lambda_3 = 535$ nm). The last channel used excitation at 430 nm and emission was recorded at 535 nm.

As the probes are structurally similar, also their metal ion affinities are not expected to lead to a very analyte-selective response, but rather a cross-reactive one.^[7] In the response data (Figure 4A), the dark colors (purple and black) in the heatmap correspond to negative intensity values and indicate fluorescence quenching while the lighter colors (yellow and white) indicate amplification. Testing the discriminatory capability of the attosensor array was performed using statistical multivariate methods, such as linear discriminant analysis (LDA) (Figure 4B).^[8,7] These approaches are routinely used to interpret and evaluate the responses from cross-reactive sensor arrays, providing a graphical output useful to gain an insight into the clustering of the response data, and to calculate classification accuracy.^[8,9] LDA show 100 % correct classification and reflect analyte-specific quenching amplification and absorption–emission shifts due to varying metal electropositivity.^[9]

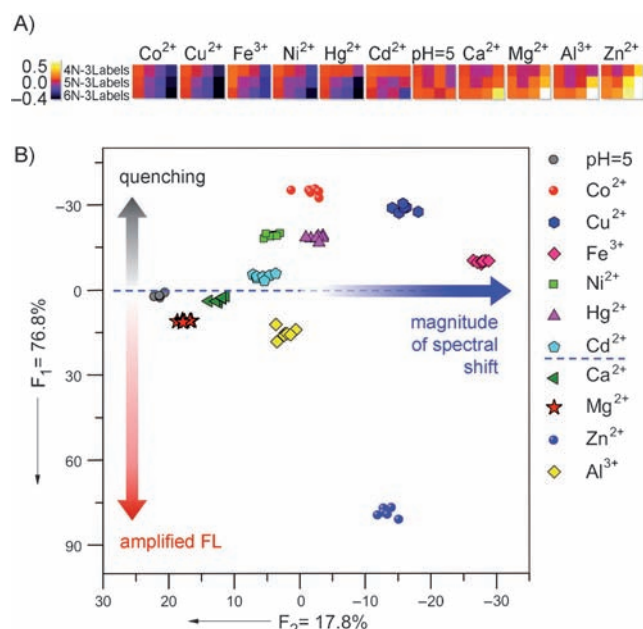


Figure 4. The response to metal ions recorded from the nanofiber arrays. A) Response heatmap: The fluorescence changes induced by the metal ions in four emission channels show the evolution of the signals (quenching/amplification), suggesting high variance in the response. B) The linear discriminant analysis (LDA) shows a clear clustering of the analytes.

The attosensor mats also provide quantitative information regarding the metal ion content. In our preliminary experiments, we used the 12×12 mm mats and deposited 200 nL droplets of analyte of increasing metal concentration. The changes in fluorescence were recorded as described above to give intensity vs. concentration graphs (response isotherm, see Supporting Information for examples). For example, in the 200 nL samples, the lowest limit of detection for Co^{2+} ions was 2.0 ppm and for Zn^{2+} ions it was 3.0 ppm (in water, pH 5).

Finally, we deposited a conformal coating of the attosensors mat onto a nitrile glove using a shadow mask (Figure 5). When it was exposed to a solution of Co^{2+} ions ($20.0 \mu\text{M}$), the sensor mat showed an immediate quenching of the fluorescence. This result illustrates the scalability of the described electrospun attosensor mats including mechanical strength and a fast attosensor response, thus suggesting a potential utility in fabrication of wearable sensors that could be, for example, part of a hazmat suit.

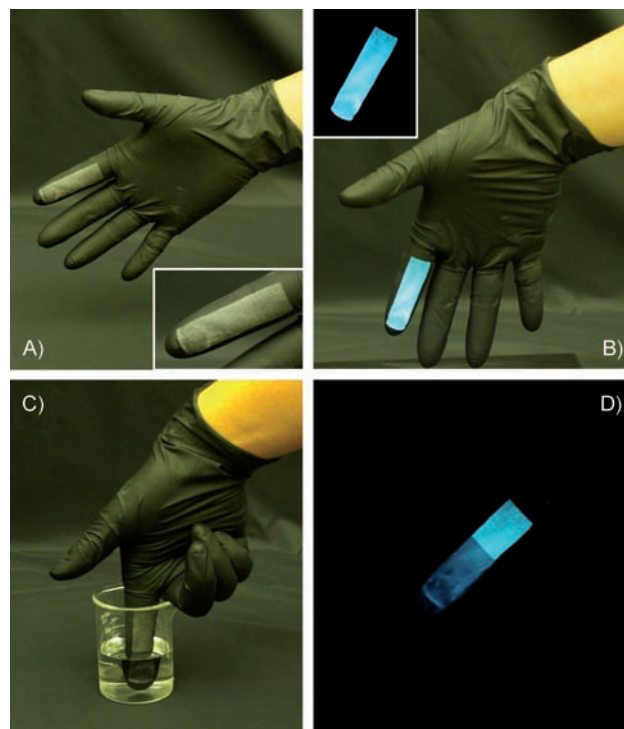


Figure 5. Attoliter reactor mats as wearable sensors: Nanofiber mat shadow mask deposited on a glove (A), its fluorescence under black light (365 nm; B), exposure to a solution of Co^{2+} ions ($20.0 \mu\text{M}$; C) resulting in fluorescence attenuation as seen under black light (D).

In summary, we have shown a simple method for fabrication of ultrasensitive fluorescent probes and their application as wavelength-addressable sensor arrays capable of qualitative and quantitative sensing of metal cations. The probes generated in situ from three label precursors and three amines were capable of identifying eleven analytes in both a qualitative and a quantitative fashion. Varying the probe concentration in each attoreactor will directly affect the dynamic range of the response of each attoreactor. The latter opens a possibility for tuning the dynamic range of response of the sensors to meet the profile of the target analyte. The sensors could be deposited on various devices and objects including protective safety wear (wearable sensors). Quantitative studies and tests of complex analytes will be performed in the near future.

Received: August 8, 2011

Revised: October 28, 2011

Published online: January 3, 2012

Keywords: attoreactors · metal ions · nanotechnology · sensors · supramolecular chemistry

-
- [1] P. Anzenbacher, Jr., M. A. Palacios, *Nat. Chem.* **2009**, *1*, 82–88.
 [2] a) D. Li, Y. Xia, *Adv. Mater.* **2004**, *16*, 1151–1170; b) W.-E. Teo, R. Inai, S. Ramakrishna, *Sci. Technol. Adv. Mater.* **2011**, *12*, 013002.
 [3] a) F. S.-J. Kim, G.-Q. Ren, S. A. Jenekhe, *Chem. Mater.* **2011**, *23*, 682–732; b) B. Ding, M. Wang, X. Wang, X. J. Yu, G. Sun, *Mater. Today* **2010**, *13*, 16–27.
 [4] C. A. Pasternack, Ed. *Monovalent Cations in Biological Systems*, CRC, Boca Raton, FL, **1990**.
 [5] a) T. R. Crompton, *Toxicants in Terrestrial Ecosystems*, Springer, Berlin, **2006**; b) T. R. Crompton, *Toxicants in Aqueous Ecosystems*, Springer, Berlin, **2006**; c) R. Dulbecco, *Encyclopedia of Human Biology*, 2nd ed., Academic Press, New York, **1997**.
 [6] L. Prodi, M. Montalti, N. Zaccheroni, *Helv. Chim. Acta* **2001**, *84*, 690–706.
 [7] a) J. J. Lavigne, E. V. Anslyn, *Angew. Chem.* **2001**, *113*, 3212–3225; *Angew. Chem. Int. Ed.* **2001**, *40*, 3118–3130; b) A. P. Umali, E. V. Anslyn, *Curr. Opin. Chem. Biol.* **2010**, *14*, 685–692; c) P. Anzenbacher, Jr., P. Lubal, P. Bucek, M. A. Palacios, M. E. Kozelkova, *Chem. Soc. Rev.* **2010**, *39*, 3954–3979; d) P. Anzenbacher, Jr., Y. Liu, M. E. Kozelkova, *Curr. Opin. Chem. Biol.* **2010**, *14*, 693–704.
 [8] R. G. Brereton, *Applied Chemometrics for Scientists*, Wiley, Chichester, **2007**.
 [9] a) C. H. Chen, J. Shi, *Coord. Chem. Rev.* **1998**, *171*, 161–174; b) M. A. Palacios, Z. Wang, V. A. Montes, G. V. Zyryanov, P. Anzenbacher, Jr., *J. Am. Chem. Soc.* **2008**, *130*, 10307–10314; c) Z. Wang, M. A. Palacios, P. Anzenbacher, Jr., *Anal. Chem.* **2008**, *80*, 7451–7459; d) Z. Wang, M. A. Palacios, G. Zyryanov, P. Anzenbacher, Jr., *Chem. Eur. J.* **2008**, *14*, 8540–8546; e) M. A. Palacios, Z. Wang, V. A. Montes, G. V. Zyryanov, B. J. Hausch, K. Jursíková, P. Anzenbacher, Jr., *Chem. Commun.* **2007**, 3708–3710.
-